Scientific Excellence • Resource Protection & Conservation • Benefits for Canadians
Excellence scientifique • Protection et conservation des ressources • Bénéfices aux Canadiens

Coupling Similarity-Modelled Surface Gravity Shallow Water Waves and the Statistical Structure of Forcing Winds

W. Perrie and B. Toulany

Physical and Chemical Sciences Branch
Scotia-Fundy Region
Department of Fisheries and Oceans

Bedford Institute of Oceanography
P.O. Box 1006
Dartmouth, Nova Scotia
Canada B2Y 4A2

March 1989

Canadian Technical Report of Hydrography and Ocean Sciences No. 115

Fisheries and Oceans Pêches et Océans

Canada

Canadian Technical Report of Hydrography and Ocean Sciences

Technical reports contain scientific and technical information that contributes to existing knowledge but which is not normally appropriate for primary literature. The subject matter is related generally to programs and interests of the Ocean Science and Surveys (OSS) sector of the Department of Fisheries and Oceans.

Technical reports may be cited as full publications. The correct citation appears above the abstract of each report. Each report is abstracted in *Aquatic Sciences and Fisheries Abstracts* and indexed in the Department's annual index to scientific and technical publications.

Technical reports are produced regionally but are numbered nationally. Requests for individual reports will be filled by the issuing establishment listed on the front cover and title page. Out of stock reports will be supplied for a fee by commercial agents.

Regional and headquarters establishments of Ocean Science and Surveys ceased publication of their various report series as of December 1981. A complete listing of these publications is published in the *Canadian Journal of Fisheries and Aquatic Sciences*, Volume 39: Index to Publications 1982. The current series, which begins with report number 1, was initiated in January 1982.

Rapport technique canadien sur l'hydrographie et les sciences océaniques

Les rapports techniques contiennent des renseignements scientifiques et techniques qui constituent une contribution aux connaissances actuelles, mais qui ne sont pas normalement appropriés pour la publication dans un journal scientifique. Le sujet est généralement lié aux programmes et intérêts du service des Sciences et levés océaniques (SLO) du ministère des Pêches et des Océans.

Les rapports techniques peuvent être cités comme des publications complètes. Le titre exact paraît au-dessus du résumé de chaque rapport. Les rapports techniques sont résumés dans la revue *Résumés des sciences aquatiques et halieutiques*, et ils sont classés dans l'index annuel des publications scientifiques et techniques du Ministère.

Les rapports techniques sont produits à l'échelon régional, mais numérotés à l'échelon national. Les demandes de rapports seront satisfaites par l'établissement auteur dont le nom figure sur la couverture et la page du titre. Les rapports épuisés seront fournis contre rétribution par des agents commerciaux.

Les établissements des Sciences et levés océaniques dans les régions et à l'administration centrale ont cessé de publier leurs diverses séries de rapports en décembre 1981. Une liste complète de ces publications figure dans le volume 39, Index des publications 1982 du *Journal canadien des sciences halieutiques et aquatiques*. La série actuelle a commencé avec la publication du rapport numéro 1 en janvier 1982.

Canadian Technical Report of

Hydrography and Ocean Sciences No. 115

March 1989

COUPLING SIMILARITY-MODELLED SURFACE GRAVITY SHALLOW WATER WAVES AND THE STATISTICAL STRUCTURE OF FORCING WINDS

by

W. Perrie and B. Toulany

Physical & Chemical Sciences
Scotia-Fundy Region
Department of Fisheries and Oceans

Bedford Institute of Oceanography
Dartmouth, Nova Scotia
Canada B2Y 4A2

90-05153/

© Minister of Supply and Services 1989
Cat. No. FS 97-18/115E ISSN 0711-6764

Correct citation for this publication:

Perrie, W. and B. Toulany. 1989. Coupling Similarity-Modelled Surface Gravity Shallow Water Waves and the Statistical Structure of Forcing Winds. Can. Tech. Rep. Hydrogr. Ocean Sci. No. 115: iv + 40 pp.

ABSTRACT

Perrie, W. and B. Toulany. 1989. Coupling Similarity-Modelled Surface Gravity Shallow Water Waves and the Statistical Structure of Forcing Winds. Can. Tech. Rep. Hydrogr. Ocean Sci. No. 115: iv + 40 pp.

Our approach to wind-generated surface gravity waves parameterizes net energy transfer due to nonlinear wave-wave interactions and wind input to waves. The wave-wave interaction term is calibrated to model the appropriate complete Boltzmann integrals and the system is assumed to evolve to a Pierson-Moskowitz/JONSWAP shape asymptotically with time. Fetch-limited and duration-limited growth curves are consistent with recent experimental results. The model is discretized in frequency and direction components and propagates according to a finite-difference scheme. Wave-growth and swell-decay events can exist simultaneously.

Shallow water is accommodated by extending Phillips' saturation range concepts both to finite depth and to the entire spectral range. The so-called Kitaigorodskii factor is applied to the spectral shape functions for growth and saturation and therefore, implicitly for swell and Phillips' original α function as well. The deep water dispersion relation, phase and group velocities are replaced by depth-dependent versions.

Directional wave buoy measurements from a two-week period in 1984 provide data for model verification and characterisation. Wind data to force the waves are derived from surface pressure data interpolated to the grid of the model. Preparation of the pressure data by spline fitting is compared with interpolation by objective analysis. The latter, using the spline fit interpolation as a first guess field, assumes a weighting for the difference between observation and first guess values which minimizes the ensemble average analysis error.

RESUME

Perrie, W. and B. Toulany. 1989. Coupling Similarity-Modelled Surface Gravity Shallow Water Waves and the Statistical Structure of Forcing Winds. Can. Tech. Rep. Hydrogr. Ocean Sci. No. 115: iv + 40 pp.

Notre modèle des ondes de gravité de surface dues au vent comporte un paramètre de transfert net d'énergie dû aux interactions vagues- vagues et un paramètre d'apport du vent à la formation de vagues. Le terme d'interaction vagues- vagues est étalonné pour

représenter les intégrales compètes de Boltzmann qui sont appropriées, et on suppose que le système prend asymptotiquement une forme JONSWAP de Pierson-Moskowitz avec le temps. Les courbes de croissance limitées en fetch et en durée concordent avec les résultats expérimentaux récents. Dans le modèle, les composantes de fréquence et de direction sont discrètes, et la propagation se fait par différences finies. Des vagues peuvent grossir pendant que la houle diminue.

On tient compte des faibles profondeurs d'eau en étendant le principe d'intervalle de saturation de Phillips aux profondeurs finies et à la gamme spectrale complète. Le facteur dit de Kitaigorodskii est appliqué aux fonctions de forme spectrale pour la croissance et la saturation et donc, implicitement, pour la houle ainsi que pour la fonction originale de Phillips. La relation de dispersion en eau profonde et les vitesses de phase et de groupe sont remplacées par des fonctions de la profondeur.

À partir de mesures d'ondes directionnelles prises à l'aide de bouées pendant une période de deux semaines en 1984, on obtient des données pour la vérification et la caractérisation du modèle. Des données d'entrainement des vagues par le vent sont obtenues à partir de données de pression en surface interpolées à la grandeur du réseau du modèle. La préparation des données de pression par ajustement d'une fonction spline est comparée à l'interpolation par analyse objective. Cette dernière, basée sur l'interpolation par ajustement d'une fonction spline comme première approximation, suppose une pondération pour la différence entre les observations et les valeurs de première approximation qui minimise l'erreur d'analyse moyenne globale.

(1) Introduction

From the balance of spectral energy from wind input, nonlinear wave-wave interactions and dissipation due to wave breaking etc., the JONSWAP experiment of Hasselmann et al (1973) demonstrated that the deep water spectral shape has a universal similarity. The generalization of this concept is due to Bouws et al (1985b) in their analysis of the wave data from the Dutch lightship TEXEL and the experiments MARSEN, in the southern North Sea, and ARSLOE, off the North Carolina coast. The resultant TMA spectral shape is a similarity form, universal in that it is site-independent, but depth-dependent. In the deep water limit this spectral form approaches the JONSWAP parameterization, its parameters becoming JONSWAP deep water parameters.

In the high frequency range, the TMA shape is the same as that obtained by Kitaigorodskii et al (1975) in extending Phillips' (1958) saturation range concepts for deep water conditions to finite depth situations. The novelty of the TMA spectrum is the application of the resultant similarity scaling factor to the entire spectral range rather than just restricting it to the equilibrium range. The theory of Kitaigorodskii et al assumes an equilibrium regime within the spectrum in which energy is transferred to higher frequencies without dissipation. This is clearly limited in frequency range and cannot explain the TMA shape, which covers all frequencies.

The SWIM study of Bouws et al (1985a) intercompared three operational shallow water wave models for two artificial experiments and a severe storm hindcast and thus tried to understand shallow water wave processes and implementations in wave models. The models were the

British Meteorological Office model BMO, of Golding(1983); GONO, the model developed at KNMI by Janssen et al (1984) for the North Sea; and HYPAS, developed in Hamburg and described in Günther and Rosenthal (1984). The hypothetical intercomparison tests were (1), fetch-limited growth due to steady offshore winds in water of constant depths 15, 30, 60, and 120m and (2), onshore winds in water of gently decreasing depth and constant slope. The hindcast test uses accurately reconstructed wind fields for North Sea storms of 18-26 November 1981 and intercompares the operational behavior of each model.

Results for the hypothetical tests are explained in terms of the shallow water processes represented in each model. However, in the measured and modelled spectra from the hindcast it is difficult to exactly isolate and identify these mechanisms. Bouws et al (1985a) suggest that future intercomparisions and verifications of wave models be more carefully designed so that clearer results may be obtained.

Perrie et al (1987) present the theory and concomitant model assembled by taking the formalism inferred by Bouws et al (1985b) in obtaining the TMA form, and applying it to a standard second generation coupled discrete deep water model. In the SWIM tests of Bouws et al (1985a), the model was seen to behave quite similar to HYPAS, which although otherwise different, has the same approach to modelling shallow water waves. The generalization is that given a second generation model, whether coupled discrete, or hybrid parametric etc., modifications for shallow water waves can be introduced by the TMA shape, Kitaigorodskii similarity factor and related concepts. Resultant model behavior will be dominated by TMA physics in shallow water wave situations. A short description of this model, which has its origins in Resio (1981), is

presented in the next section and a more detailed discussion in Perrie et al (1987).

An alternate view is that of Resio (1987), who uses a generalized treatment of geometric scaling rules of Boltzmann integrals for nonlinear wave-wave interactions to characterise the equilibrium spectra in arbitrary depth water. Assuming an equilibrium regime as in Kitaigorodskii (1983), a significant constant flux of wave energy through the equilibrium range of the spectrum is inferred . Using measured data from storm conditions, it is concluded that a dynamic balance between wind input and nonlinear wave-wave interactions dominates the spectral shape, and thus the total energy level and energy transfer to higher frequencies, for waves in water as shallow as 10m. Nonlinear flux estimates are found to give quantitative values for energy losses, whether or not equilibrium conditions prevail. This is particularly relevant for quite shallow water where nonlinear fluxes cannot preserve an equilibrium.

The scaling used by Resio (1987) to relate nonlinear wave-wave interactions in deep water to the more general finite depth situation is the similarity relation derived by Herterich and Hasselmann (1980). This is also central to the WAM model for waves on finite depth water, as described by Hasselmann et al (1987) and Janssen and Komen (1986). The essential assumption is that only a narrow band of the frequency domain in the neighbourhood of the peak need be considered to represent the nonlinear transfer and that depth is larger than one tenth of the wavelength. A more comprehensive study of the validity of this approach is under way using the data obtained during the CASP experiment, described by Anderson and Shaw (1987). For simple SWIM tests, the

Herterich and Hasselmann (1980) similarity as implemented in the WAM model, is quite different from the TMA form as implemented in a contemporary second generation discrete spectral model such as presented by Perrie et al (1987).

The wave observations reported here are from a single Datawell Wavec pitch-roll wave buoy moored 32.5km from the southwest tip of Nova Scotia at 43.2°N, 65.8°W adjacent to Browns Bank in 59m depth, as shown in Figure 1. In contrast to the extended sloping planar regions used in the SWIM study of Bouws et al (1985a), the MARSEN experiment or the ARSLOE experiment, Browns Bank is a plateau surrounded by irregular topography.

Preparation of the wind fields forcing the waves provides a problem in interpolation of sparse data to the grid of the wave model. A first guess is obtained by biharmonic spline fitting data from surface pressure charts at sea level, ships of opportunity and land based meteorological stations. More sophisticated ways to approach the problem include the optimal statistical objective analysis techniques, recently developed in meteorology. As will be seen in the following sections, it matters how this analysis is done and there are implications on the statistical structure of the wind fields.

Optimal statistical objective analysis (OSOA), as developed by Bengtsson and Gustavsson (1971), Rutherford (1972), Schlatter (1975), Thiébaux (1973, 1975, 1977, 1986) and many others, is the most versatile, comprehensive and powerful of the objective analysis algorithms. Optimality comes from correctly analyzing the assumed homogeneous isotropic covariance structure of the variable such that the variance of analysis error is minimized. Ensemble averaged statistics on

analysis accuracy in independent realizations are optimal in the sense that no other analysis technique can do better. OSOA is suboptimal if second-order statistics of the analyzed variable are not homogeneous, if the stochastic behavior of the increment field is not Gaussian, or if the data cannot be actually used. In application, OSOA is inescapably less than optimal because it isn't possible to match the spatial structure defining the analysis algorithm with the true spatial structure of a given analysis situation. The failure to match comes from assuming homogeneity when it isn't exactly there. The amount by which the matching fails and suboptimality prevails, results from the averaging of diverse synoptic situations in deriving the statistical structure. In this study, a lack of matching comes from applying a generally defined global spatial structure for surface level pressure fields to the analysis situation off Cape Sable where wind data are quite sparse and pressure data are on coarse scale. And yet, we see a competitor to other approaches to the analysis.

(2) Modelling Waves in Shallow Water

The starting point for understanding energy balance for wind generated surface gravity waves is numerical integration of the balance equation for action density N,

$$\frac{\partial N}{\partial t} + \frac{\partial \omega}{\partial k} \circ \frac{\partial N}{\partial x} - \frac{\partial \omega}{\partial x} \circ \frac{\partial N}{\partial k} = S = S_{in} + S_{nl} + S_{ds} + S_{b}$$

The two-dimensional surface wave spectrum F is related to action density by,

$$N = F/\sigma$$

where $F(k,x,t)$ is dependent on wavenumber k, position x, and time t, $\omega = \sigma + \underline{k} \circ \underline{U}$, where $\underline{U}$ is a slowly varying current, g is gravitational acceleration, $k = |\underline{k}|$, and $\sigma(k) = (gk \tanh kD)^{1/2}$ (D is depth) is the dispersion relation for surface gravity waves. This study neglects $\underline{U}$, so that $\omega = \sigma$. Source terms include wind input S_{in}, nonlinear transfer by wave-wave interactions S_{nl}, dissipation by wave-breaking, whitecapping or other turbulent processes S_{ds} , and dissipation by bottom processes S_b.

We use the second generation coupled discrete model described in Perrie et al (1987), as categorized by Allender et al (1985) in the SWAMP study. It predicts energy levels for discrete frequency and direction intervals and uses a finite-difference scheme to model propagation effects (exactly as in BMO). Dissipation is handled implicitly by requiring that the spectrum asymptotically approaches a JONSWAP form in time-independent wind situations. Although windsea-swell interactions are not completely understood, the formulation of the model allows simultaneous wave-growth and swell-decay events within the same region. Energy transfer due to nonlinear wave-wave interactions is parameterized to resemble the Boltzmann integrals in Hasselmann and Hasselmann (1981). Wind input is functionally consistent with Snyder et al (1981). The resultant discrete spectral model is able to reproduce the fetch-limited results of Hasselmann et al (1976) and fits well within the envelope of experimental curves for duration-limited growth.

For shallow water ($|\underline{k}| \circ D \leq 1.5$) not in the surf zone, TMA spectral concepts as given in Bouws et al (1985b), are applicable. The

frequency and depth dependent factor of Kitaigorodskii et al (1975), used to extend Phillips' deep water equilibrium range concepts to shallow water, is applied to the complete spectrum. In this manner the universal similarity shape of JONSWAP for growing waves in deep water is extended to finite depth, and the associated quasi-equilibrium approximation is made. As field data considered by Bouws et al (1985b) do not indicate dependence on bottom parameters, it is assumed that for a given frequency, dissipation in deep water varies monotonically with wavenumber and causes the variation of TMA shape with depth.

The so-called Kitaigorodskii factor,

$$\phi(\omega_D) = \frac{k(\omega,D)^{-3} \; \partial k(\omega,D)/\partial f}{k(\omega,\infty)^{-3} \; \partial k(\omega,\infty)/\partial f}$$

where f is frequency, $\omega = 2\pi f$, and $\omega_D = 2\pi f(D/g)^{1/2}$, scales growth and saturation shape functions, and thus implicitly modifies swell released from generation areas. The more general dispersion relation,

$$\omega^2 = gk \tanh kD$$

replaces the deep water relation and similarly for phase and group velocities. Dissipation for the swell regime is modelled following JONSWAP, refraction for windsea follows Golding (1983).

(3) Optimal Statistical Objective Analysis

Technical aspects of multivariate optimal interpolation have been thoroughly covered in recent literature and only a few comments are

needed here. Basic principles and definitions may be found in cited papers. A field variable at a gridpoint, such as the surface pressure field, estimated as Y_o , can be expressed as the sum of a first guess X^f_o at the specified gridpoint, and an interpolated analysis error Y'_o for this gridpoint. Letting o index the point for which the estimate is made and $1,..,j,..,m$ index gridpoints of the array, the latter may be expressed as a linear combination of anomalies X'_j for any of m observing locations,

$$Y'_o = w_1 X'_1 + \ldots + w_m X'_m$$

The coefficients w_j are derived from the covariance structure of the anomaly field so as to minimize the variance of the analysis error Y'_o, and are therefore determined solely by the covariance structure of the vector field,

$$(w_1 \ldots w_m) = (\sigma_{01} \ldots \sigma_{0m})\sigma^{-1}$$

where

$$\sigma = \begin{bmatrix} \sigma_{11} \cdots & \sigma_{1m} \\ \vdots & \vdots \\ \sigma_{m1} & \cdots \sigma_{mm} \end{bmatrix}$$

and the scalar elements σ_{ij} are covariances among all variables for locations (i,j).

It is never possible to know all the covariances from the data, especially on a regular grid. Thus, with the assumptions of temporal and spatial isotropy, simple statistical models are typically constructed so

that coefficients for Y'_o may be represented as a space-lag correlation function $\rho(s)$, where s is the geographic separation between the grid point and a measuring station,

$$(w_1 \quad \dots \quad w_m) = \left[\rho(s_{01}) \quad \rho(s_{02}) \quad \dots \quad \rho(s_{0m}) \right] \Sigma^{-1}$$

and any representation of noise to signal ratio is neglected,

$$\Sigma = \begin{bmatrix} 1 & \rho(s_{12}) & \dots & \rho(s_{1m}) \\ \rho(s_{21}) & 1 & \dots & \rho(s_{2m}) \\ \vdots & & & \\ \rho(s_{m1}) & \rho(s_{m2}) & \dots & 1 \end{bmatrix}$$

We ignore any seasonal variation and use an isotropic second-order autoregressive model space-lag correlation function,

$$R(s) = R_o \left[\cos(as) + (c/a)\sin(as) \right] e^{-cs}$$

where

$R_o = 0.96$

$a = 1.41$

$c = 0.567$

In modelling the geopotential correlation at 500mb, this was found to have the smallest sum of squared deviations from computed correlations of various forms tried by Thiébaux (1977, 1986). Similarity in the vertical dimension allows application of this analysis to pressure

fields at sea level. Thence, autocorrelations and cross- correlations involving the wind are derived from derivatives of the height field through a planetary boundary layer model. The properties and fit of these derivatives, synonomous with wind statistics, constrain their usefulness in multivariate interpolation schemes.

(4) The Storm Situation of 17-26 November 1984

(a) Introduction

The test of any numerical simulation wave model is how well it represents the complex and interacting processes that exist in a real geophysical situation. A conclusion in Bouws et al (1985a) is that it is always difficult to isolate a simple hypothetical test in a real situation and to infer model performance and ability.

The wave model of this study has been explored via the SWIM tests in Perrie et al (1987). The storm events chosen here, 17-26 November 1984, were selected by two basic criteria: availability of reliable shallow water wave measurements, and of the numerically reconstructed wind fields over a large enough area using the methods presented here. At the time of this writing the chosen storms were those first identified as meeting these requirements.

(b) The Meteorological Situation

The meteorological situation of 17-26 November 1984 is dominated first by the presence of a weak low extending from the Gulf of St.

Lawerence to Lac Saint-Jean, Quebec. This intensifies slightly, moves eastward over Newfoundland and by November 18, joins the much more intense Labrador low which then deepens and propagates east. Our analysis of concomitant surface winds, presented in the following section, concludes that initially moderate westerlies at ≈ 10m/s, intensify slightly and veer to the southeast.

A second low begins developing over Maine and propagates over the Bay of Fundy and Cape Breton Island by November 19. Extending along the coast as far south as North Carolina, it associates with a cold front, which develops along the coast from Long Island to the Bay of Fundy and moves offshore to the southeast. Consolidating and propagating further eastward beyond Newfoundland by November 20, this second low interacts with more intense lows in the mid-North Atlantic. We infer that surface wind fields continue turning and become northerlies, intensifing to ≈ 15m/s by 12GMT on November 21.

Meanwhile a developing high over the Great Lakes gains strength and moves eastward reaching Scotian Shelf by November 23. Wind fields weaken somewhat and become more westerly.

The following event is an evolving low over Labrador which moves southeast to Newfoundland and is associated with a cold front along the continental shelf off Nova Scotia. In turn, the latter moves eastward reaching Flemish Cap by November 24. Associated winds change direction once more, becoming northerlies with a maximum of about 15m/s.

Finally, a high extending from West Virginia intensifies and reaches Nova Scotia by November 26. Our analysis gives an increasingly westerly component to the winds.

Wind data taken from a bow-mounted anemometer on CSS Dawson, which

was within 100km of the directional wave buoy, are shown in Figure 2. Since the observed scale of prevailing weather patterns greatly exceeded 100km and since Dawson was beyond the zone where winds are significantly influenced by the land (a few km; Smith and MacPherson, 1987), these winds are representative of the area surrounding the wave buoy.

(c) Processing the Wind Data

Subjectively drawn sea surface pressure charts of the Canadian Atmospheric Environment Service at the Atlantic Weather Centre (plotted on a regular polar stereographic projection grid at 00Z, 06Z, 12Z and 18Z daily), ship of opportunity records and land based meteorological stations result in about 30 pressure observations in each 40°- 50°N by 50°- 70°W meteorological map. We apply two-dimensional spline fitting to these to obtain pressure fields for the wave model grid, as in Figures 3(a) and (b) for 12 GMT and 18 GMT on November 17 respectively. Using the empirical and analytical meteorological relations of the Cardone (1969) planetary boundary layer model, first guess surface wind fields are generated to drive the wave model, as in Figure 4(a) and (b). Subsequently Figures 3(c) and (d), and 4(c) and (d) show the application of optimal statistical objective. Comparing wind fields and pressure fields gives a measure of the approximation that is being made in either technique. While not as close as that of the North Sea SWIM hindcast study, the comparison of observed and modelled wind fields is favourable, with the difference in magnitude generally within 25%, and direction, 35°.

(d) The Measured Wave Data

Significant wave height H_s, mean period $\bar{T}$ and mean wave direction $\bar{\theta}$ are computed from the one-dimensional spectrum $F(f)$ and two-dimensional spectrum $F(f,\theta)$, by the relations,

$$H_s = 4\,(m_0)^{1/2} \qquad \bar{T} = m_0/m_1$$

$$\bar{\theta} = \text{Arg}\left[\frac{1}{m_0}\int_0^{\infty}\int_0^{2\pi} e^{i\theta}\; F(f,\theta)\; df\; d\theta\right]$$

where moments of the spectrum are given by

$$m_n = \int_{.05}^{0.5} f^n\; F(f)\; df \quad .$$

Confidence limits for H_s and $\bar{\theta}$ depend on the number of degrees of freedom of the spectral estimates as in Long (1980). We estimate the 90% confidence limits for H_s to be 0.85 and 1.23 times the expected value of H_s; for $F(f)$, to be 0.72 and 1.51 times the expected value of $F(f)$; and for $\bar{\theta}$, to be $\pm 10^{\circ}$.

(e) Model Operational Characteristics

We have discussed the physical and mathematical basis of the wave model in previous sections. Our concern here is with the operational characteristics of the model as implemented in this study. The grid

network is shown in Figure 5, where spatial resolution is 55.5km and timestep, 0.5hr. Wave frequencies are discretized from 0.03 to 0.22Hz in increments of 0.01Hz and represented by a parametric regime thereafter. Directional resolution is 22.5^{o} and the open boundary specification is that energy flux be zero. A criticism may be that the area is rather small for a viable modelling of waves given this grid. The area was chosen to make the best of a sparse dataset. Extending it would not have forseeably enhanced the density of data nor the modelling effort.

The TMA parameterization of Bouws et al (1985b) implies that the Wavec is in comparably deep water and that much of the time the waves do not feel the bottom. The coarseness of the grid in Figure 5 is a further limitation on modelling as large topographical scale features are represented and small scale structures ignored.

Finally, the complexity of the wind fields is only known to the extent that data is available. Mesoscale structure that is not in this dataset cannot be modelled in spline fit or objective analysis wind fields, leading to situations in the wave model that are improperly modelled and possibly overpredicted.

(f) Results of the Model Hindcast

For the period November 17-26, the wave dataset is not complete, but three peaks from storm events contained within that period were recorded. Time series plots for H_s, $\overline{T}$ and $\overline{\theta}$, for measurements and model results, are shown in Figures 7-8. Observed maxima were 4.0m on the 17th, 3.6m on the 21th and 3.8m on the 24th, although the first two peaks were probably higher.

Concerning the first storm (November 17-18), the model approximately locates the time and to some extent the magnitude of the event. As indicated in Figure 7, wave heights estimated from wind fields derived from spline fitting seem to model the peak well, although the absence of data exactly at the peak makes it difficult to assess. Results from optimal statistical objective analysis, as shown in Figure 8, generally overestimate wave heights while still locating the peak and qualitatively following the measured data. The two-dimensional energy spectrum from the buoy, as obtained using the method of Long (1980) and Long and Hasselmann (1979) for November 17 at 12 GMT and 18 GMT, are respectively Figures 9(a) and (b). The model result from winds derived from spline fitting are respectively Figures 9(c) and (d). The winds derived from OSOA analysis lead to Figures 9(e) and (f) respectively. Both efforts are poor in estimating the peak frequency. Figures 9(e) and (f) are better than 9(c) and (d) at estimating the direction at the peak.

The spectra leading to the second peak are modelled approximately. The energy level is correct both when spline fit wind fields are used and also when the wind fields are objectively analyzed. Smaller details of the spectra are modelled qualitatively with some lag.

In some regard, the second storm of Novovember 21 repeats much of what is seen in the first. The location of the peak is indicated, and the details and magnitude of the peak are poorly represented. Wave heights from objective analysis wind fields are not as good as those from spline fit wind fields.

Thereafter both modelling efforts overestimate the spectral energy level in observations leading to the final storm peak. To a large

degree, this results from inaccurate ship of opportunity pressure data and thus wind fields that are too high and too complex. The passage of a cold front on November 24, mentioned in section 4(b) and not treated in the wind analysis, results in the failure of both efforts to locate the third peak correctly. Interestingly, both modelling efforts exhibit similar features, with the spline fitting method generally slightly less than results from objective analysis.

Regarding $\overline{T}$, results from either spline fit wind fields or objectively analyzed wind fields are closer to observations than the H_s comparison. Generally the spline wind fields do well, indicating the location of the first and second peaks and missing the third peak. The OSOA wind fields result in an overall match to the measured data, providing the location of all three peaks while overpredicting them.

Smaller scale variation is suppressed in subjectively drawn surface pressure maps, which are smoothed to the scale of the observations. Spline fitting may introduce further smoothing, as does OSOA. In situations where fetch is limited by wind variations, all these lead to an overestimate in fetch - especially in localized storms.

Comparison of measured directional behavior with modelling efforts is also presented in Figures 7-8. The changing wind direction events of November 19, 20, 23 and 26 are reflected in wave data on about these same days. The results from objectively analyzed winds are lagged with respect to the data. Spline fit winds give waves able to respond to wind direction changes, with some lag. Figure 6 and Wavec data not shown here imply that low frequency energy arriving from outside the Browns Bank study area and not reproduced in the model is obscured by locally generated windsea.

Overall statistics are in Table 1, showing that shallow water effects are present throughout the study, although slight. Spline fitting gives good agreement with observed H_s data whereas OSOA leads to results which are acceptable and consistently poorer. For $\bar{T}$ data, OSOA offers a modest improvement over spline fitting.

An extensive manual and computer analysis was carried out on the meteorological data. However major errors undoubtably remain simply because the data are very sparse and it is impossible to know the wind fields accurately. Directional error is undoubtably a major source of the poor modelling. The very short fetch to the coast from the directional buoy means that when the wind blows offshore the grid representation of Figure 5 is not accurate and the model does poorly. This happens in its failure to more accurately deal with the second peak. Had there been sufficient data it would have been possible to more carefully model the covariance functions implicit in forcing wind fields.

(5) Conclusions

The primary aim of this paper was to test approaches to modelling waves in shallow water, to gain an understanding of the mechanisms at work and the ways in which they interact. There are two aspects to what has been done here.

Firstly, the shallow water model constructed by taking a standard second generation discrete spectral wave model and implementing the TMA formalism of Bouws et al (1985b) has been tested on Wavec data in a highly irregular coastal area. This is in contrast to the gently varying

environs from which the TMA dataset was collected. The basic model responds reasonably to meteorological forcing, although had both wind and wave data been more plentiful, a more definitive comparison would have been possible.

Secondly, this has been a study of the preparation of wind fields and the sensitivity of the model on wind field preparation and structure. Optimal statistical objective analysis should be an enhancement on wind preparation for wave modelling. That it was not, is a reflection on the paucity of the data and the rather general covariance functions. These were derived on very broadly based datasets with wide application and coherence lengths that do not represent the current study.

Clear aspects that emerged from the study are;

(a) The basic shallow water model successfully reproduced the various levels of wave energy in the measured data. Maximum and minimun energy levels in high and low wind speed are acceptably reproduced with some shallow water reduction when the wind has an onshore component.

(b) Growth of spectral energy is correctly modelled, although modelling of rapidly turning wind fields and other aspects have yet to be properly represented, as follows from Figures 7-8.

(c) Excessive growth levels in fetch- and duration-limited situations, as seen on November 17 and 21 in Figure 7, are a shortcoming. These reflect the shape functions for growth within the model, which were calibrated against other models via the hypothetical SWAMP tests by Perrie and Toulany (1985).

(d) The covariance function used in our objective analysis is

clearly not the best choice. In the situation where data is sufficiently abundant, a better approach would be the direct computation of covariance function structure. Objective analysis would then use spline fit surface pressure fields as the first guess field.

Acknowledgements

We gratefully acknowledge comments from Fred Dobson, Peter Smith and Stu Smith. The dataset would not have been available were it not for the CSS Dawson crew, Physical and Chemical Sciences technicians at BIO and especially Jim Murphy at the Marine Environmental Data Service who oversaw the data collection and preliminary processing. Wave modelling at BIO is funded by the Office of Energy Research and Development.

References

Allender J. H., Barnett T. P., Bertotti L., Bruinsina J., Cardone V. J., Cavaleri L., Ephraums J. J., Golding B., Greenwood A., Guddal J., Günther H., Hasselmann K., Hasselmann S., Joseph P., Kawai S., Komen G. J., Lawson L., Linne H., Long R. B., Lybanon M., Maeland E., Rosenthal W., Toba Y., Uji T. and W. J. P. de Voogt (1985) 'Sea Wave Modelling Project (SWAMP): An intercomparison study of wind-wave prediction models, Part 1- Principal results and conclusions'. Proc. IUCRM Symp. on Wave Dynamics and Radio Probing of the Ocean Surface, Miami, Plenum.

Anderson, C. and R. Shaw (1987) The Canadian Atlantic Storms Program (CASP): An Overview. Proc. International Workshop on Wave Hindcasting and Forecasting, Bedford Inst., Dartmouth, Nova Scotia, 1986.

Bengtsson, L. and N. Gustavsson (1972) Assimilation of nonsynoptic observations. Tellus, 24, 383-399.

Bouws E., Ephraums J. J., Komen G. J., Rosenthal W. and W. J. P. de Voogt (1985a) 'A shallow water intercomparison of three numerical wave prediction models (SWIM)'. Quart. J. R. Met. Soc. 111, 1087- 1112.

Bouws, E., Günther, H., Rosenthal, W. and C. L. Vincent (1985b) Similarity of the wind wave spectrum in finite depth water, Part 1 - Spectral form. J. Geophys. Res. 90, 975-986.

Cardone, V. J. (1969) Specification of the wind distribution in the marine boundary layer for wave forecasting. Tech. Rep. 69-1, Geophys. Sci. Lab., New York University, 137 pp.

Golding, B. W. (1983) A wave prediction system for real time sea state forecasting. Quart. J. R. Met. Soc. 109, 393-416.

Günther, H. and W. Rosenthal (1984) A shallow water surface wave model based on the TEXEL-MARSEN-ARSLOE (TMA) wave spectrum. Proc. 20th Congress IAHR, Moscow, 1983.

Hasselmann, K., Barnett, T. P., Bouws, E., Carlson, H., Cartwright, D. E., Enke, K., Ewing, J. A., Gienapp, H., Hasselmann, D. E., Kruseman, P., Meerburg, A., Müller, P., Olbers, D. J., Richter, K., Sell, W. & Walden H. (1973) Measurements of wind-wave growth and swell decay during the Joint North Sea Wave Project (JONSWAP) Dt. hydrogr. Z., A8 (suppl.), no. 12, 95pp.

Hasselmann, K., Ross, D. B., Müller, P. and W. Sell (1976) A parametic wave prediction model. J. Phys. Oceanogr. 6, 200-228.

Hasselmann, S. and K. Hasselmann (1981) A symmetrical method of computing the nonlinear transfer in a gravity-wave spectrum. Hamb. Geophys. Einzelschriften, Reihe: Wiss. Abhand., 52, 138 pp.

Hasselmann, S., Hasselmann, K., Janssen, P. A. E. M., Komen, G. J., Bertotti, L., Guillaume, A., Cardone,V. J., Greenwood, A., Reistad, M. and J. A. Ewing (1987) The WAM model, a third generation ocean wave prediction model. In preparation.

Herterich, K. and K. Hasselmann (1980) A similarity relation for the nonlinear energy transfer in a finite-depth gravity-wave wave spectrum. J. Fluid Mech. 97, 215-224.

Janssen, P. A. E. M. and G. J. Komen (1986) A shallow water extension of the 3-G WAM model. KNMI Tech. Memo.

Janssen, P. A. E. M., Komen, G. J. and W. J. P. de Voogt (1984) An operational coupled hybrid wave prediction model. J. Geophys. Res. 89, (c3), 3635-3654.

Kitaigorodskii, S. A. (1983) On the theory of the equilibrium range in the spectrum of wind-generated gravity waves. J. Phys. Oceanogr. 13, 816-827.

Kitaigorodskii, S. A., Krasitskii, V. P. & M. M. Zaslavskii (1975) On Phillips' theory of equilibrium range in the spectra of wind-generated gravity waves. J. Phys. Oceanogr., 5, 410-420.

Long, R. B. (1980) The statistical evaluation of directional spectrum estimates derived from pitch/ roll buoy data. J. Phys. Oceanogr., 10, 944-952.

Long, R. B. and K. Hasselmann (1979) A variational technique for extracting directional spectra from multicomponent wave data. J. Phys. Oceanogr., 9, 373-381.

Perrie, W. and B. Toulany (1985) Assessing a wave model à la SWAMP. Can. Tech. Rep. Hydrogr. Ocean Sci., 67, vi+78 pp.

Perrie, W., Günther, H., Rosenthal, W., and B. Toulany (1987) Modelling wind generated surface gravity waves using similarity. Submitted to Quart. J. R. Met. Soc.

Phillips, O. M. (1958) The equilibrium range in the spectrum of wind-generated waves. J. Fluid Mech. 4, 426-434.

Resio, D. T. (1981) The estimation of a wind wave spectrum in a discrete spectral model. J. Phys. Oceanogr., 11, 510-525.

Resio, D. T. (1987) Shallow water waves I: Theory. J. Waterway, Port, Coastal and Ocean Engineering, 113 (3), 266-283.

Rutherford, I. D., (1972) Data assimilation by statistical interpolation of forecast error fields. J. Atmos. Sci., 29, 809-815.

Schlatter, T. W. (1975) Some experiments with a multivariate statistical objective analysis scheme. Mon. Weather Rev., 105, 1465-1468.

Snyder, R. L., Dobson, F. W., Elliott, J. A., and R. B. Long (1981) Array measurements of atmospheric pressure fluctuations above surface gravity waves. J. Fluid Mech., 102, 1-59.

Smith, P. C. and J. I. MacPherson (1987) Cross-shore variations of near- surface wind velocity and atmospheric turbulence at the land-sea boundary during CASP (1987) Atmosphere-Ocean, 25, 279-303.

Thiébaux, H. J. (1973) Maximally stable estimation of meteorological parameters at grid points. J. Atmos. Sci., 30, 1710-1714.

Thiébaux, H. J. (1975) Experiments with correlation representations for objective analysis. Mon. Weather Rev., 103, 617-627.

Thiébaux, H. J. (1977) Extending estimation accuracy with anisotropic interpolation. Mon. Weather Rev., 105, 691-699.

Thiébaux, H. J., Mitchell, H. L. and D. W. Shantz (1986) Horizontal structure of hemispheric forecast error correlations for geopotential and temperature. Mon. Weather Rev., 114, 1048-1066.

TABLE 1. Verification Statistics for the Wave Model

N		71		
$\langle H_s (m) \rangle$		2.05		
$\langle \bar{T} (s) \rangle$		5.74		
Model	(1)	(2)	(3)	(4)
Model depth (m)	∞	∞	20	20
Mean height error (m)	0.29	1.34	0.25	1.19
Difference RMS (m)	-0.01	0.42	-0.01	0.41
Scatter index	-0.37	20.47	-0.46	19.76
No. of +ve errors	45	60	42	58
No. of -ve errors	26	11	29	13
Mean period error (s)	0.49	1.37	0.46	1.23
Difference RMS (s)	-0.29	-0.14	-0.30	-0.12
Scatter index	-4.98	-2.40	-5.22	-2.05
No. of +ve errors	48	60	46	61
No. of -ve errors	23	11	25	10

where

N = number of observations

$\langle H_s \rangle$ = mean of observed significant wave heights

$\langle \bar{T} \rangle$ = mean of observed periods

Difference RMS = model RMS height minus observed RMS height

$$\text{Scatter index} = 100 \times \frac{\text{difference RMS}}{\text{mean observations}}$$

and

(continued)

(1) - second generation coupled discrete deep water wave model with winds derived from spline fit surface analysis

(2) - as (1) with winds derived from OSOA surface analysis

(3) - as (1) with TMA shallow water wave formalism

(4) - as (3) with winds derived from OSOA surface analysis

FIGURE CAPTIONS

Figure 1. Local topography of Browns Bank off the southern tip of Nova Scotia showing the location of the directional wave buoy ⊗ Depth contours are 50m ~·~·~ , 100m ~·~, 200m ~ and 1000m ~~.

Figure 2. Bow anemometer wind data from the Dawson.

Figure 3. Surface pressure maps at sea level over the Gulf of Maine - Scotian Shelf on 17 November 1984 at: (A) 12 GMT and (B) 18 GMT from spline fitting and (C) 12 GMT and (D) 18 GMT from objective analysis.

Figure 4. Examples of numerically reconstructed winds corresponding to the pressure maps in Fig. 3 with (A) and (B) from spline fitting and (C) and (D) from objective analysis.

Figure 5. The hindcast computation grid showing depth contours (50m ~·~·~ , 100m ~·~, 1000m ~~).

Figure 6. Overview of the 1-dimensional wave spectra from the directional wave buoy showing elements of the low-frequency swell.

Figure 7. Time series of significant wave height H_s, mean wave period $\bar{T}$, and mean wave direction $\bar{\theta}$, for measurements+++ and model•••. Two-dimensional spline fitting is used in analysis of surface charts to derive the wind fields.

Figure 8. As Fig. 7. Wind fields are derived from optimal statistical objective analysis using the spline fitted results as first guess.

Figure 9. Two-dimensional energy spectrum on 17 November 1984 at 12 GMT and 18 GMT respectively for: (A) and (B), buoy measurements, (C) and (D), model results with winds derived from spline fitting and (E) and (F), model results derived from OSOA.

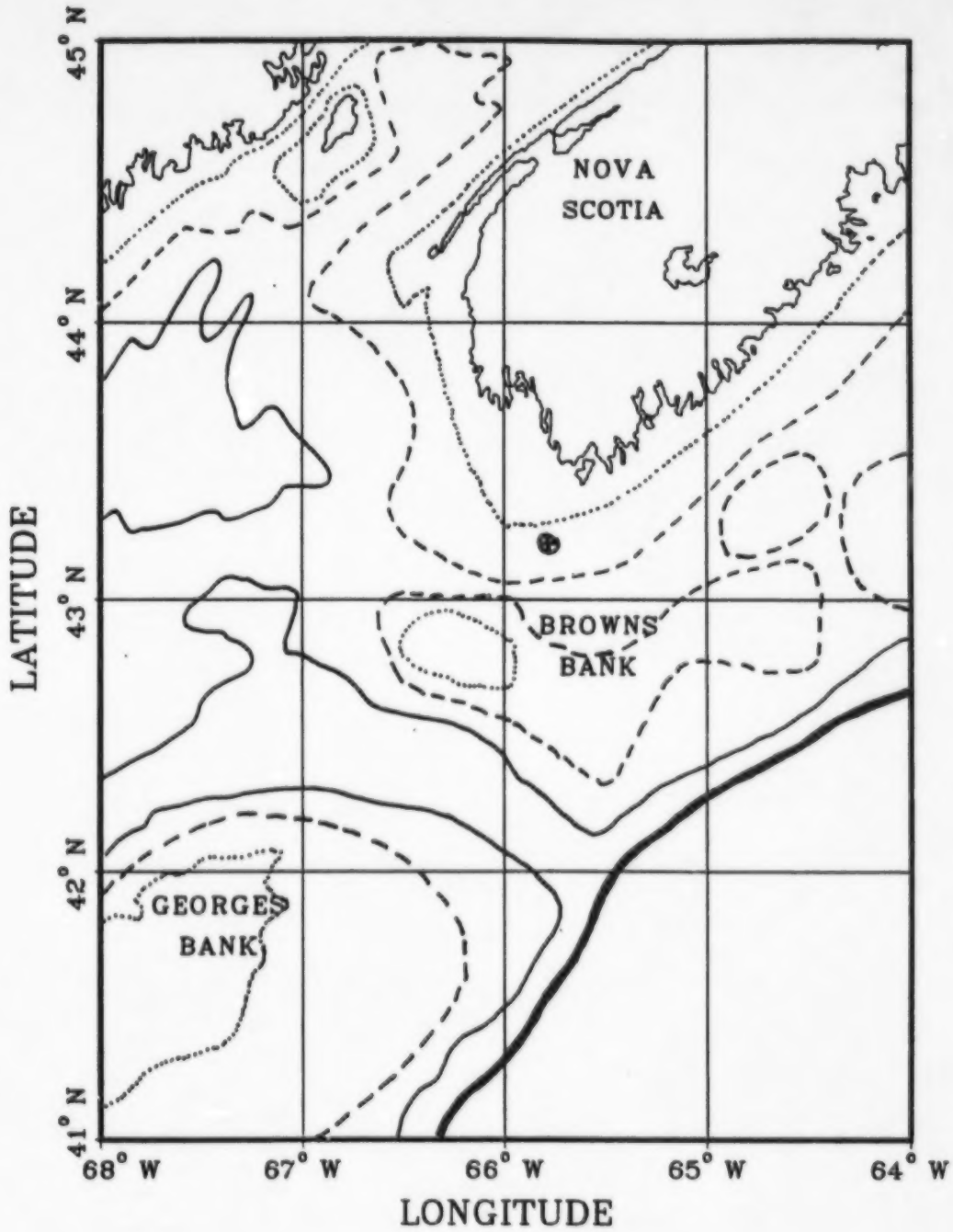

Figure 1. Local topography of Browns Bank off the southern tip of Nova Scotia showing the location of the directional wave buoy ● . Depth contours are 50m ⌒, 100m ⌒, 200m ⌒ and 1000m ⌒.

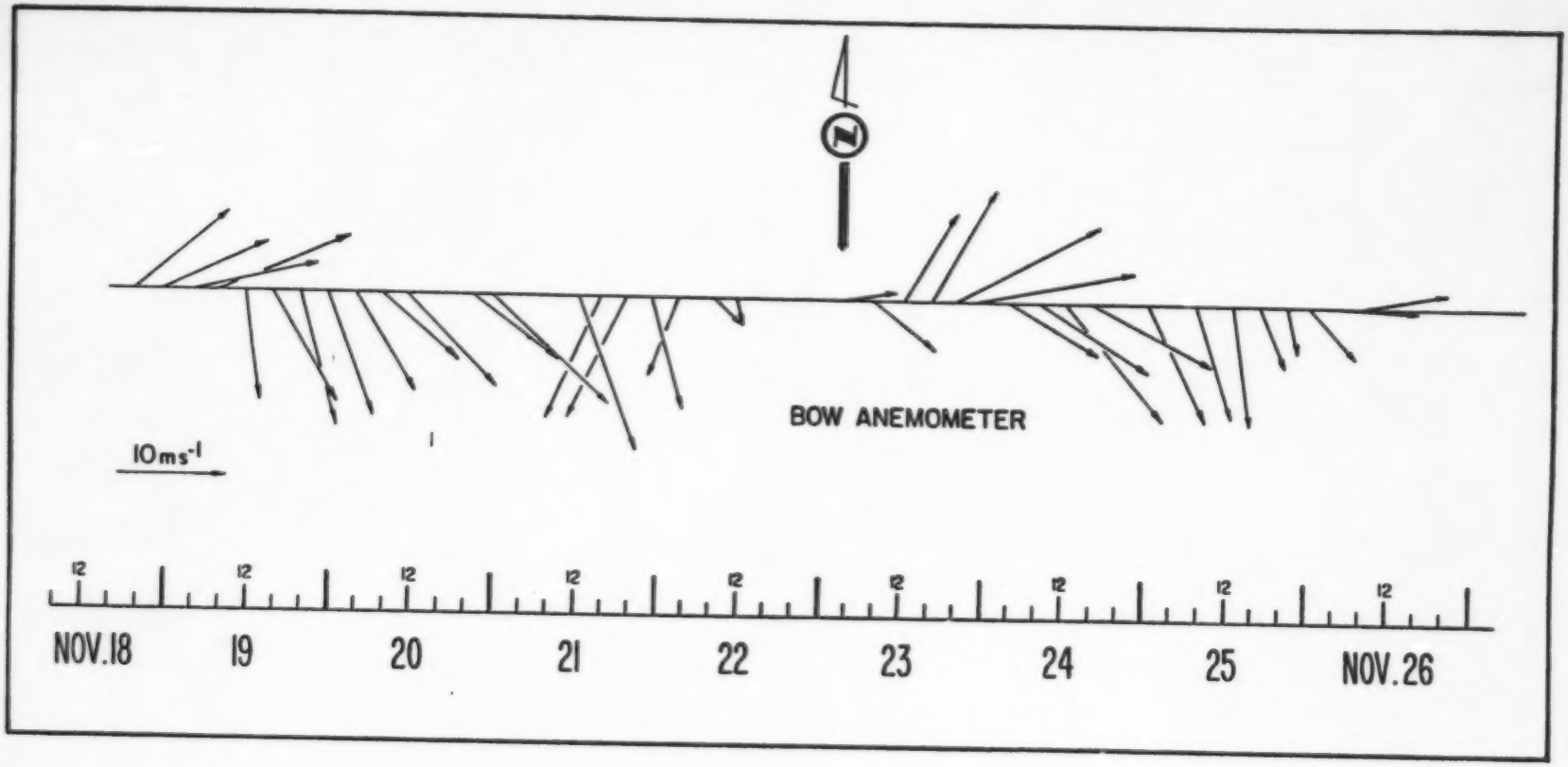

Figure 2. Bow anemometer wind data from the Dawson.

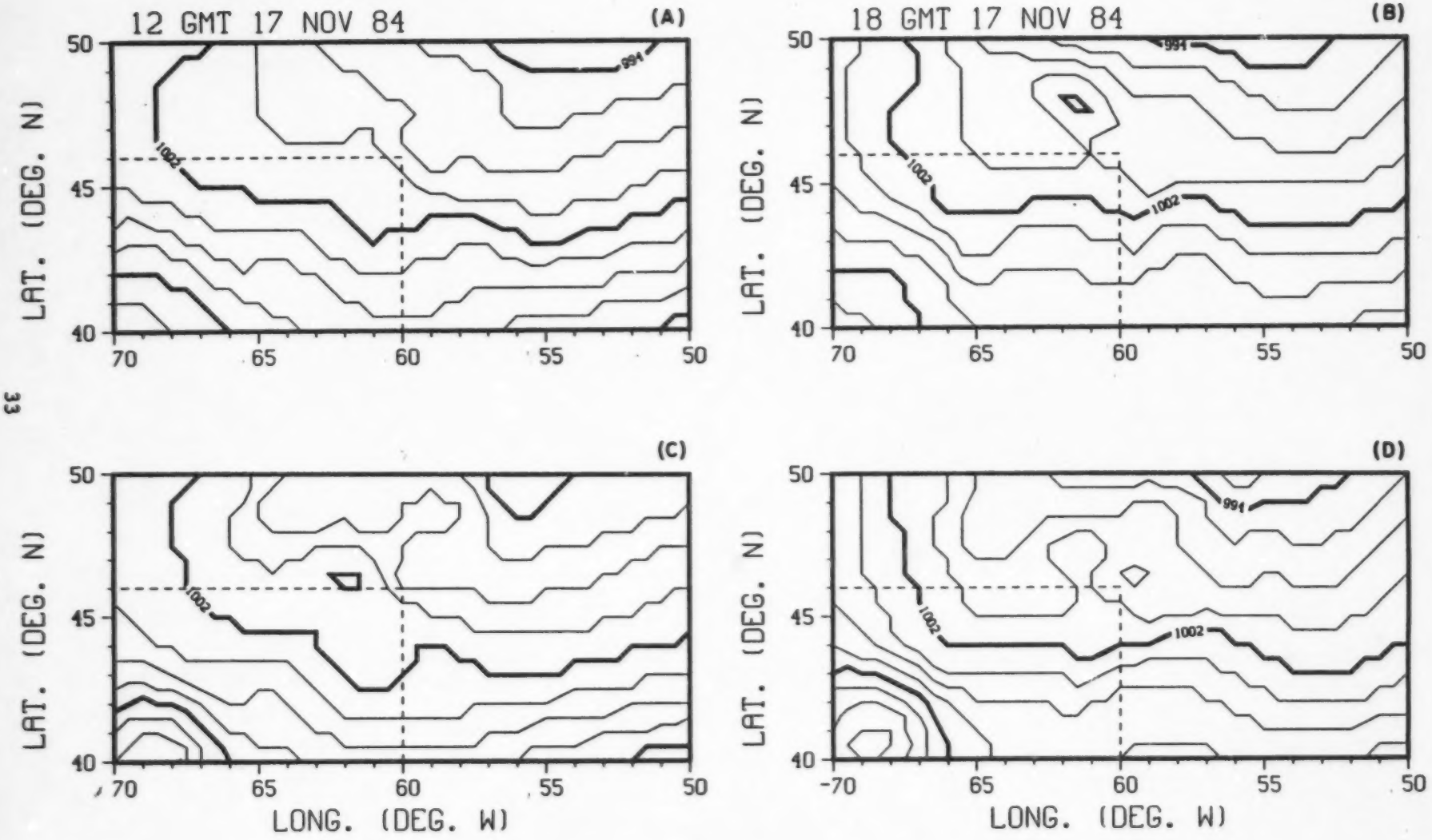

Figure 3. Surface pressure maps at sea level over the Gulf of Maine - Scotian Shelf on 17 November 1984 at: (A) 12 GMT and (B) 18 GMT from spline fitting and (C) 12 GMT and (D) 18 GMT from objective analysis.

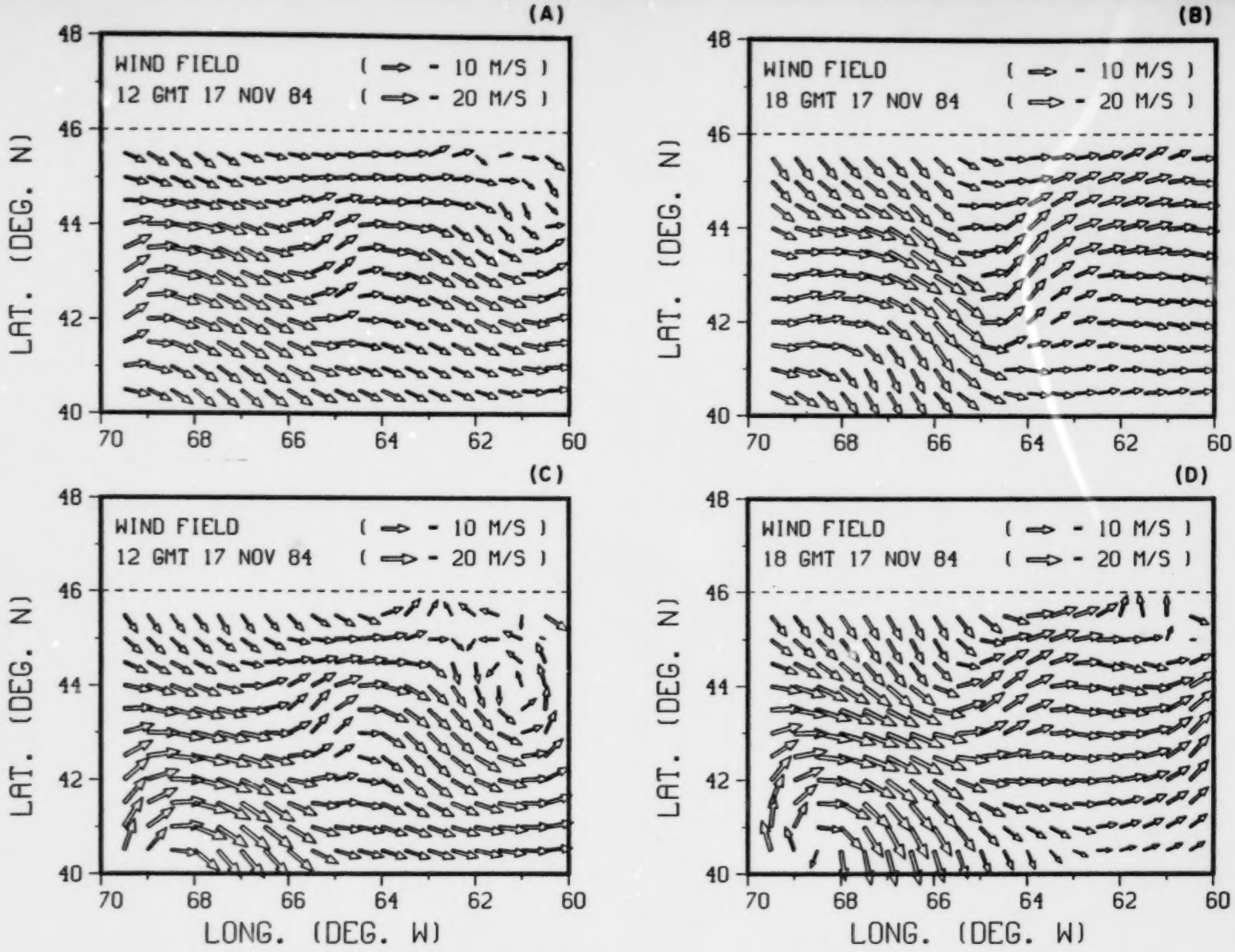

Figure 4. Examples of numerically reconstructed winds corresponding to the pressure maps in Fig. 3 with (A) and (B) from spline fitting and (C) and (D) from objective analysis.

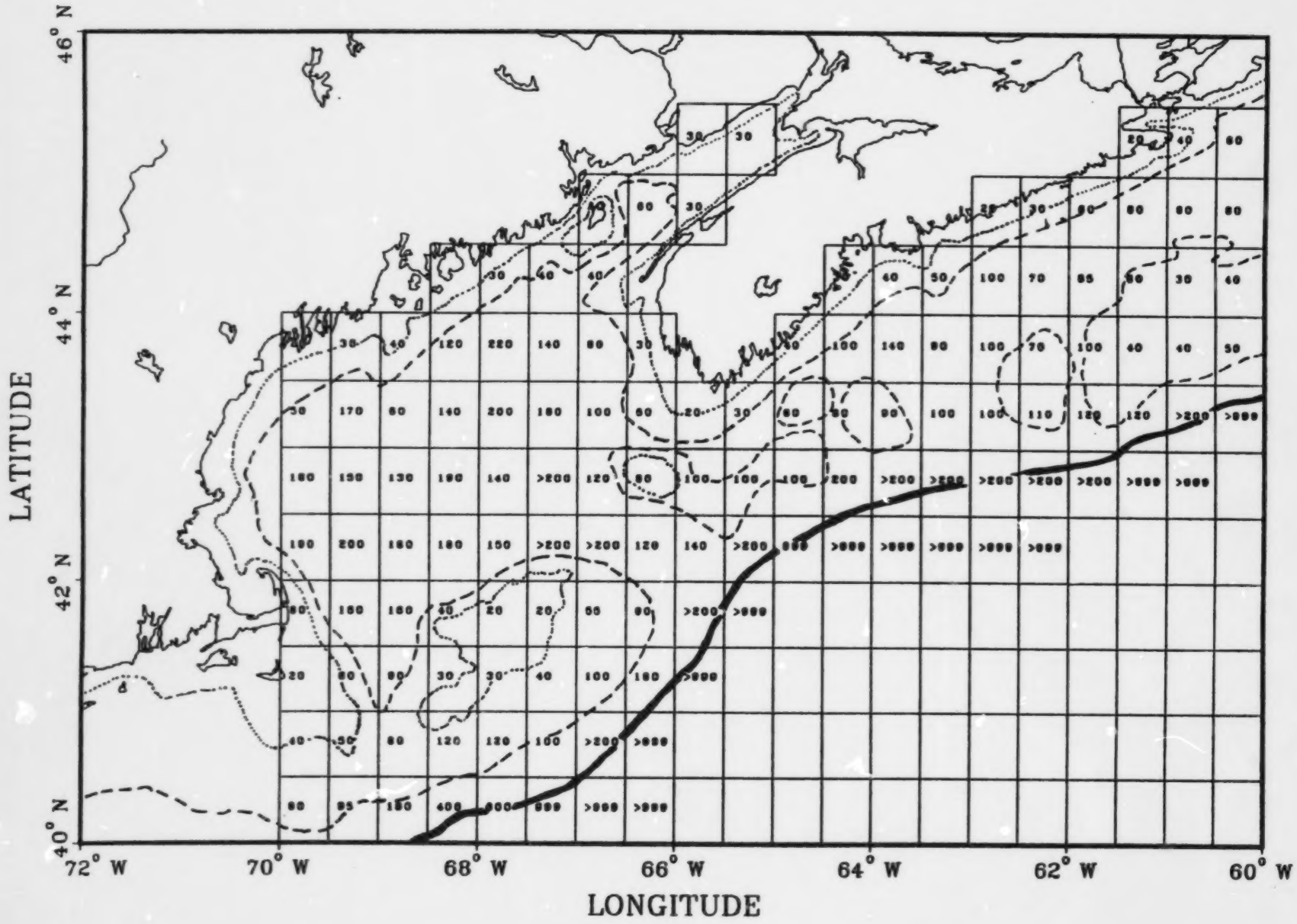

Figure 5. The hindcast computation grid showing depth contours (50m ····· , 100m – – , 1000m ▬).

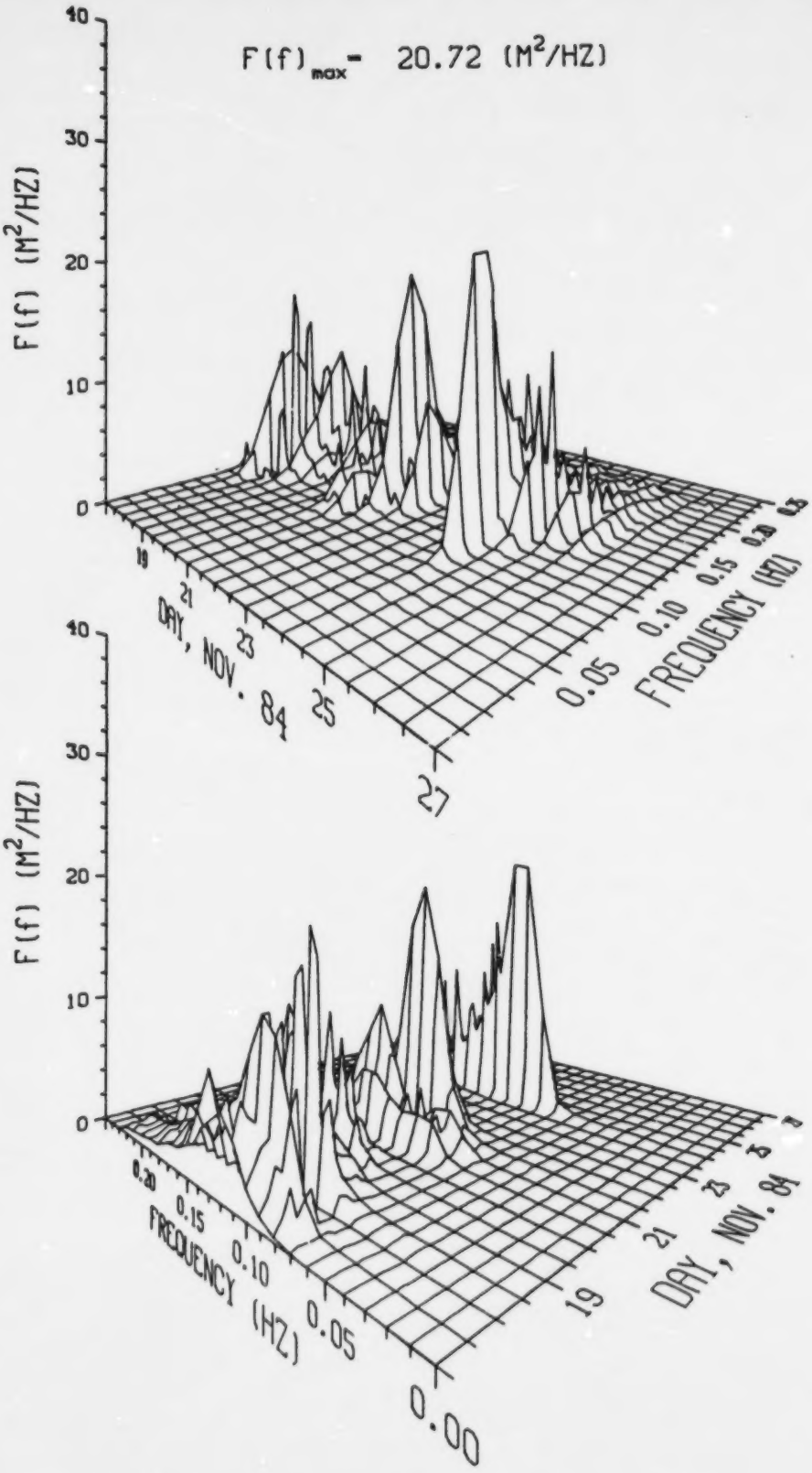

Figure 6. Overview of the 1-dimensional wave spectra from the directional wave buoy showing elements of the low-frequency swell.

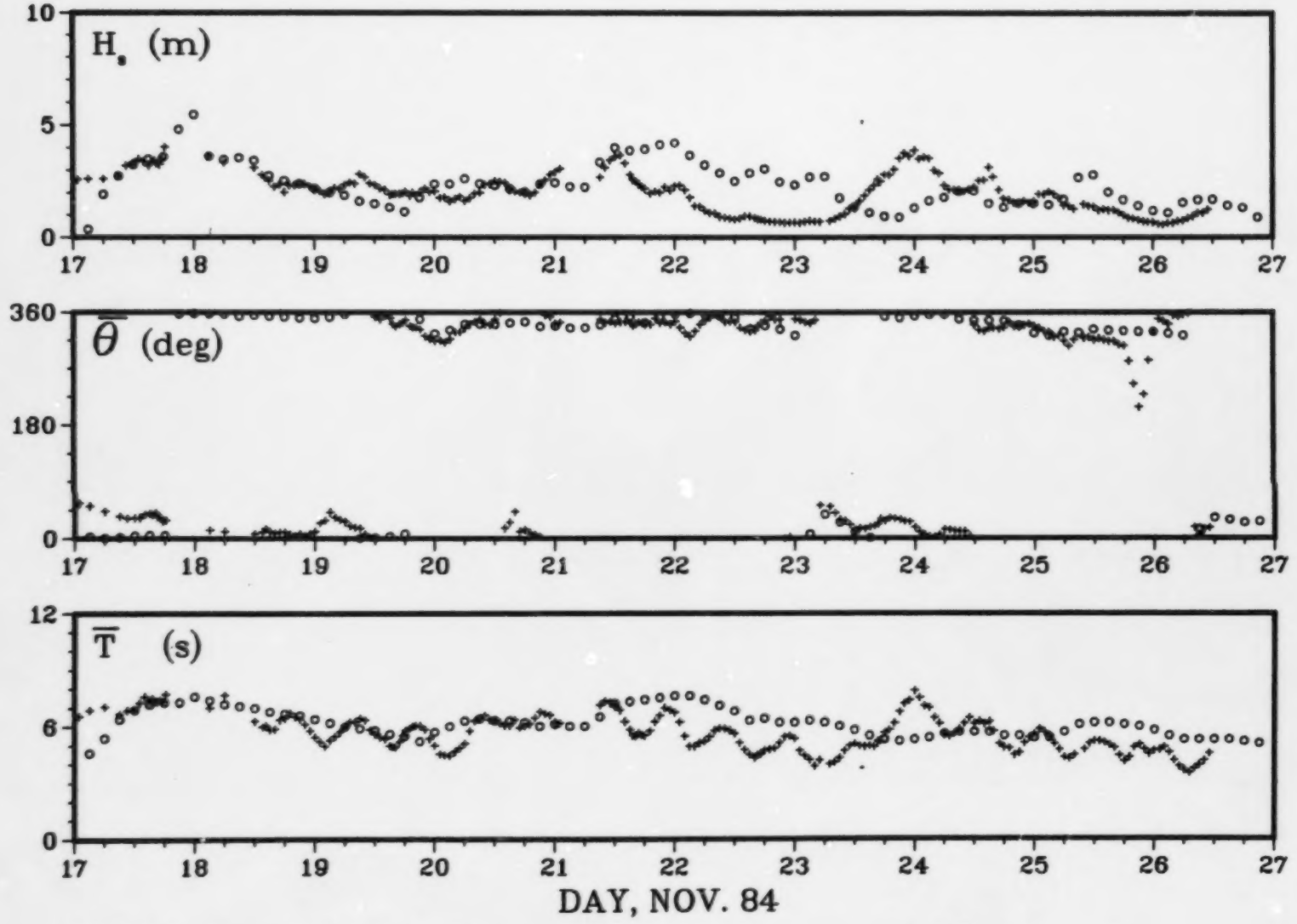

Figure 7. Time series of significant wave height H_s, mean wave period $\bar{T}$, and mean wave direction $\bar{\theta}$, for measurements+++ and model---. Two-dimensional spline fitting is used in analysis of surface charts to derive the wind fields.

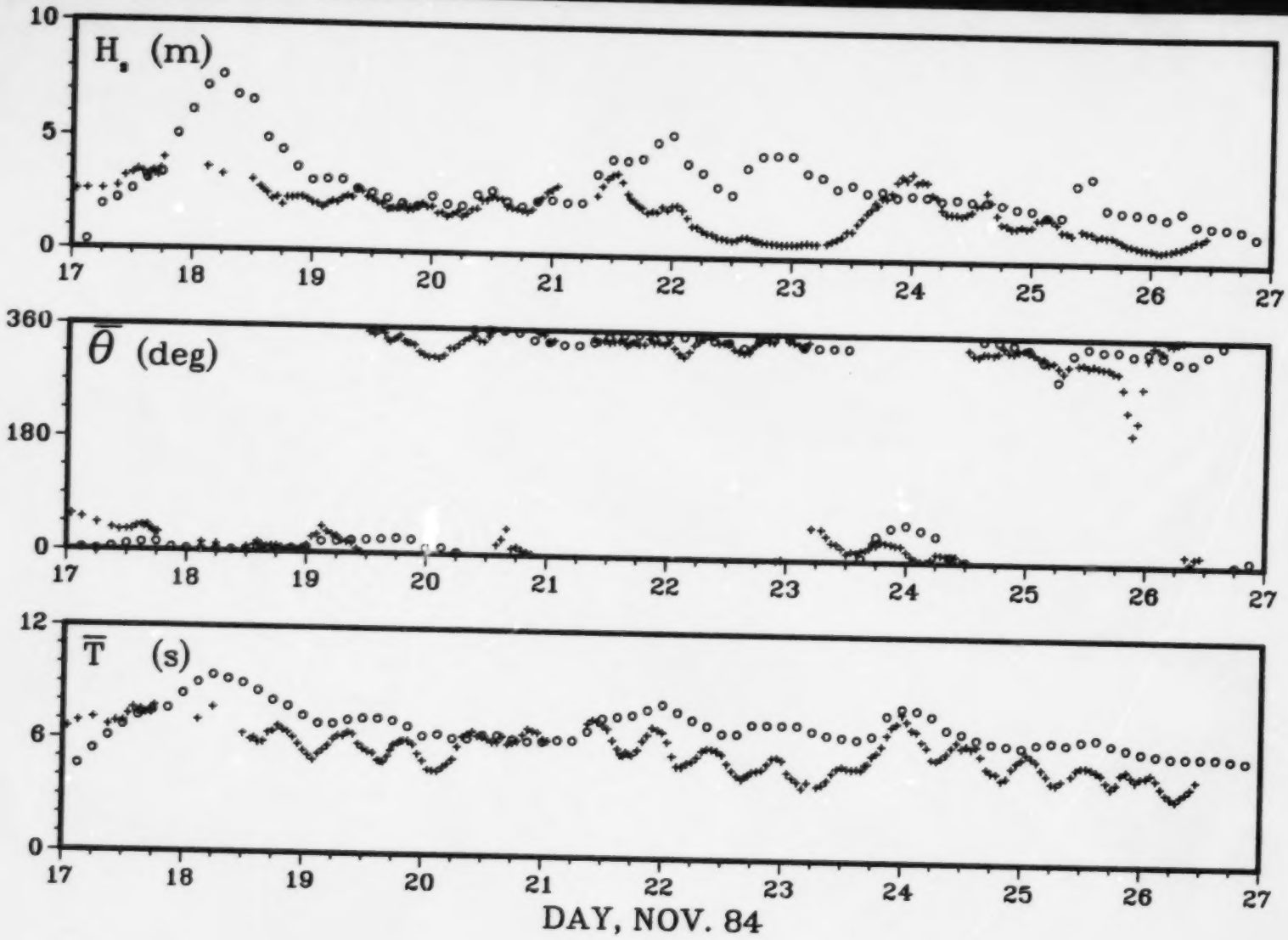

Figure 8. As Fig. 7. Wind fields are derived from optimal statistical objective analysis using the spline fitted results as first guess.

Figure 9. Two-dimensional energy spectrum on 17 November 1984 at 12 GMT and 18 GMT respectively for: (A) and (B), buoy measurements, (C) and (D), model results with winds derived from spline fitting and (E) and (F), model results derived from OSOA.

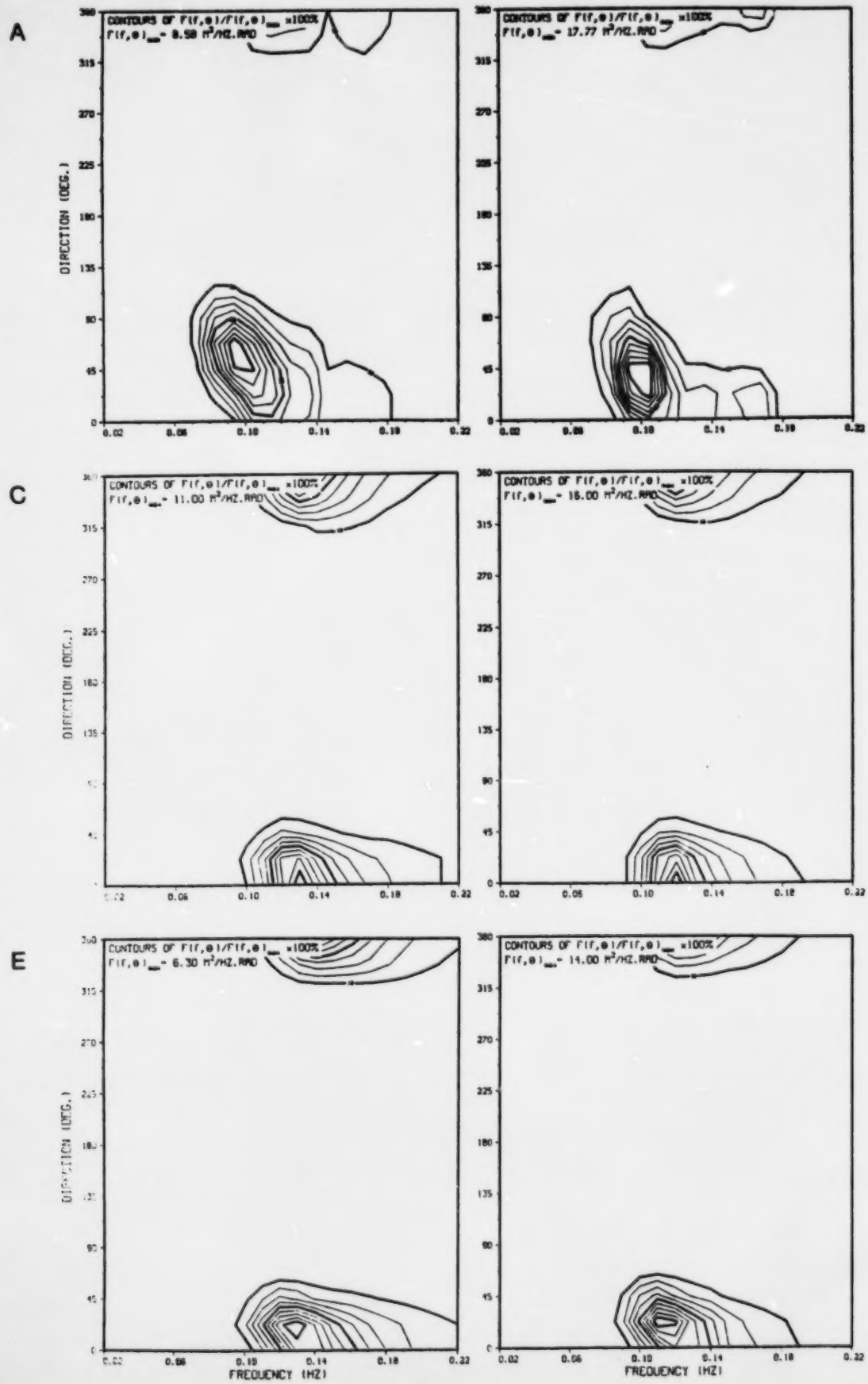
A
B
C
D
E
F
CONTOURS OF F(f,θ)/F(f,θ)__ ×100%
F(f,θ)__ = 8.58 M²/HZ.RAD
F(f,θ)__ = 17.77 M²/HZ.RAD
F(f,θ)__ = 11.00 M²/HZ.RAD
F(f,θ)__ = 16.00 M²/HZ.RAD
F(f,θ)__ = 6.30 M²/HZ.RAD
F(f,θ)__ = 14.00 M²/HZ.RAD
DIRECTION (DEG.)
FREQUENCY (HZ)
0.02
0.06
0.10
0.14
0.18
0.22
0
45
90
135
180
225
270
315
360